EXTENDED REPORT

Ultrahigh resolution optical coherence tomography in non-exudative age related macular degeneration

C G Pieroni, A J Witkin, T H Ko, J G Fujimoto, A Chan, J S Schuman, H Ishikawa, E Reichel, J S Duker

Br J Ophthalmol 2006;**90**:191–197. doi: 10.1136/bjo.2005.076612

See end of article for authors' affiliations

Correspondence to: Elias Reichel, MD, New England Eye Center, Tufts-New England Medical Center, Tufts University, 750 Washington Street, Box 450, Boston, MA 02111, USA; ereichel@tufts-nemc.org

Accepted for publication 2 October 2005

Aim: To describe the appearance of the non-exudative forms of age related macular degeneration (AMD) as imaged by ultrahigh resolution optical coherence tomography (UHR-OCT).

Methods: A UHR-OCT ophthalmic imaging system, which utilises a femtosecond laser light source capable of ~3 μm axial resolution, was employed to obtain retinal cross sectional images of patients with non-exudative AMD. Observational studies of the resulting retinal images were performed.

Results: 52 eyes of 42 patients with the clinical diagnosis of non-exudative AMD were imaged using the UHR-OCT system. 47 of the 52 (90%) eyes had the clinical diagnosis of drusen and/or retinal pigment epithelial (RPE) changes. In these patients, three patterns of drusen were apparent on UHR-OCT: (1) distinct RPE excrescences, (2) a saw toothed pattern of the RPE, and (3) nodular drusen. On UHR-OCT, three eyes (6%) with a clinical diagnosis of non-exudative AMD had evidence of fluid under the retina or RPE. Two of these three patients had findings suspicious for subclinical choroidal neovascularisation on UHR-OCT.

Conclusion: With the increased resolution of UHR-OCT compared to standard OCT, the involvement of the outer retinal layers are more clearly defined. UHR-OCT may allow for the detection of early exudative changes not visible clinically or by angiography.

Age related macular degeneration (AMD) is the leading cause of irreversible blindness in industrialised countries.[1 2] The pathogenesis of AMD is not well understood, but progression from early to advanced stages has been documented, beginning with the appearance of drusen. The diagnosis of drusen is based on biomicroscopic fundus examination findings. Drusen are categorised according to size, consistency, and the appearance of their boundaries. Large (>63 μm), amorphous, ill defined soft drusen and confluent drusen are more likely to progress to advanced AMD, in contrast with discrete, well demarcated, hard drusen.[3 4] Histologically, drusen are described as either basal laminar deposits between the plasma membrane and the basement membrane of the RPE or basal linear deposits located in the inner collagenous layer of Bruch's membrane.[5 6]

Exudative AMD, a form of advanced AMD, is characterised by the formation of choroidal neovascularisation initially under the RPE resulting in clinical findings such as subretinal haemorrhage, subretinal fluid, retinal oedema, RPE detachments, and, eventually, disciform scarring. Current treatment practices are guided by the results of the Macular Photocoagulation Study (MPS), the Treatment of Age-Related Macular Degeneration with Photodynamic Therapy Study (TAP) trial and the Pegaptanib for Neovascular Age-related Macular Degeneration Study. The diagnosis of exudative AMD and the approach to treatment are driven by angiographic findings. The best outcomes are usually in those patients whose pathology is detected early and in whom the lesions are small.[7–15]

Recently, a ultrahigh resolution optical coherence tomography (UHR-OCT) ophthalmic imaging system has been demonstrated to allow an axial resolution of 2–3 μm.[16] The increase in resolution over standard OCT reveals greater detail of the retinal layers, particularly at the level of the external limiting membrane and the photoreceptor inner/outer segment junction (IS/OS).[17] Other authors have also identified the highly reflective layer formerly thought to be part of the RPE/choriocapillaris complex as a component of the neurosensory retina.[18 19]

We developed a UHR-OCT system capable of retinal imaging and have obtained UHR-OCT images from 42 patients with the clinical diagnosis of dry AMD, including drusen, retinal pigment epithelium (RPE) changes, and geographic atrophy. The objective of this study was to identify the features of these forms of macular degeneration as imaged by UHR-OCT. Given the improvement in axial image resolution, UHR-OCT may reveal features of dry AMD that provide information about the pathogenesis of this disease and aid its characterisation and management beyond the scope of slit lamp biomicroscopy or fluorescein angiography. Perhaps, high risk characteristics for progression to exudative AMD can be identified that may become useful as new treatments become available.

METHODS

The axial resolution of OCT has an inverse relation to the optical bandwidth of the light source used for imaging.[20 21] Whereas standard OCT uses superluminescent diodes emitting light in the range of 20–30 bandwidths at 800 nm, allowing for 10–15 μm resolution, our UHR-OCT uses a state of the art titanim:sapphire (Ti:sapphire) laser with a 125 nm bandwidth at 815 nm centre wavelength enabling axial resolution of ~3 μm. This prototype instrument has been described previously.[22] The prototype UHR-OCT meets the safety requirements and is well within the safe retinal exposure limits as determined by the American National Standards Institute (ANSI).[23]

Abbreviations: AMD, age related macular degeneration; CNV, choroidal neovascularisation; IS, inner segment; OCT, optical coherence tomography; OS, outer segment; RPE, retinal pigment epithelium; UHR-OCT, ultrahigh resolution optical coherence tomography; VEGF, vascular endothelial growth factor

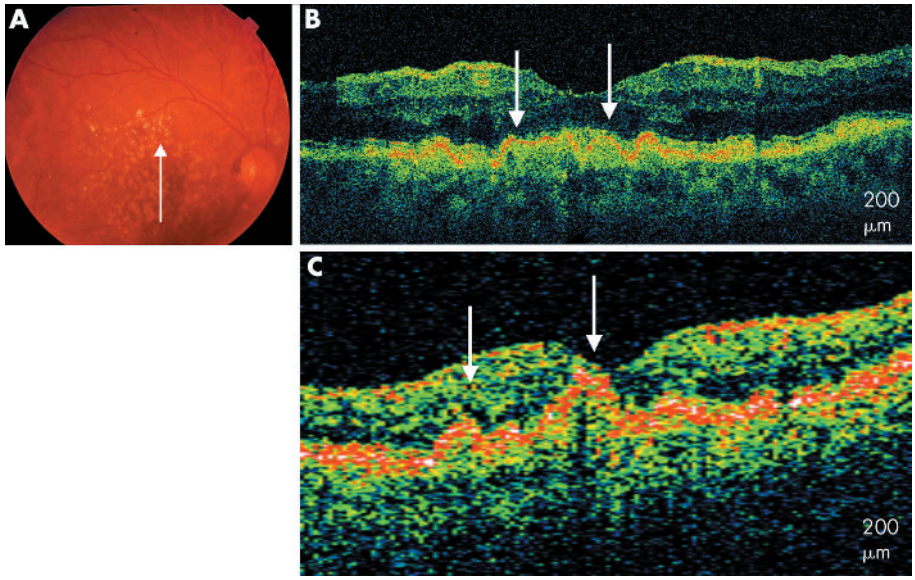

Figure 1 Soft drusen. (A) Colour fundus photograph of the right eye shows soft drusen. (B) UHR-OCT image of the right eye shows RPE excrescences with underlying moderately reflective material (white arrows). (C) StratusOCT image of the right eye with similar, less distinct modulations (white arrows).

The UHR-OCT images were generated using a 1.5 mm axial depth and 6 mm transverse width. Resolution is about 3 µm in axial direction and 15–20 µm in the transverse direction. Each UHR-OCT image consists of 3000 axial and 600 transverse pixels, and takes ~4 seconds to acquire. Similar to the StratusOCT macular imaging protocol, six 6 mm scans of the macula were obtained each separated by 30 degrees.[22] After OCT imaging was completed, all UHR-OCT images were corrected for axial motion using standard re-registration algorithms. These algorithms have been used in all of the previous prototype and commercial OCT systems.[24] The StratusOCT images are usually not corrected for axial motion because the commercial software exports only uncorrected raw images. Since the StratusOCT can acquire an image in ~1.3 seconds compared to ~4 seconds for the UHR-OCT system, the axial motions in the StratusOCT images are usually not significant; however, we have also developed software to correct the raw StratusOCT images in cases where axial motion is substantial.

The study was reviewed and approved by the institutional review board of both the Massachusetts Institute of Technology and Tufts-New England Medical Center and is compliant with the Health Insurance Portability and Accountability Act of 1996 (HIPAA). All patients signed a consent form after the nature of the study was fully explained.

Forty two patients who were examined at the New England Eye Center between November 2002 and August 2004 agreed to participate in the study. Clinical diagnoses of dry AMD were determined by slit lamp biomicroscopic findings and fluorescein angiography when indicated. Digital photography was used to document fundus findings. Patients with other macular pathologies such as diabetic macular oedema, central serous chorioretinopathy, and inflammatory conditions that could alter the interpretation of images were excluded from the study. Both StratusOCT and UHR-OCT were used to obtain cross sectional images of the macula in patients with non-exudative AMD. The resulting images were reviewed by the authors.

RESULTS

Fifty two eyes of 42 patients, aged 54–88, with a clinical diagnosis of non-exudative AMD, were imaged with UHR-OCT; 39 of the 52 eyes (75%) had the clinical diagnosis of drusen. Of the 39 eyes with drusen, three patterns were observed on the UHR-OCT images. Fifteen eyes (29%) had UHR-OCT images characterised by RPE excrescences overlying moderately reflective material consistent with drusen. RPE clumping was also apparent on the images. These findings are similar to those seen on StratusOCT but in much finer detail with clear distinction between the RPE and the overlying highly reflective junction between the inner and outer segments. Overlying theses excrescences, there were areas of compression of the photoreceptors including the inner and outer segments and outer nuclear layer (fig 1).

Another pattern, visible on UHR-OCT images of eight eyes (15%), resembled a saw toothed configuration of the RPE with multiple excrescences in succession, suggesting a wrinkling or bunching of the RPE. Moderately reflective material was visible under these excrescences. Thinning of the overlying photoreceptor layer including the outer nuclear layer and the inner and outer segments was also evident. The inner retinal layers appeared generally intact (fig 2).

A third pattern, predominant in 13 eyes (25%), was characterised by nodular, discrete drusen. These drusen did not appear as excrescences of the RPE but as disruptions of the RPE with accumulations of moderately reflective and highly reflective material. These collections appeared to correspond with hard drusen visible clinically. There is focal compression of the outer retinal layers above these nodules (fig 3).

The UHR-OCT images of three eyes (6%) with a clinical diagnosis of drusen revealed low scattering areas below the RPE consistent with presence of fluid (figs 4 and 5). These areas of pigment epithelial detachment were also visible on StratusOCT images. However, in two of the three eyes, the axial image resolution of the UHR-OCT image revealed disruptions of the RPE with areas of well defined, moderately backscattering clumping of the RPE at, above or below the level of the RPE. These RPE disruptions were associated with the hyporeflective areas of fluid suggesting the possibility of the presence of a CNV (fig 4D) These findings are present but less clearly apparent on StratusOCT images (fig 4E).

Eight eyes (15%) with clinical findings characterised predominantly by RPE changes were also imaged. These images showed clumping of hyper-reflective material at the level of the RPE. Four of these eyes revealed hyper-reflective particles in the inner retinal layers suggestive of RPE migration (fig 6).

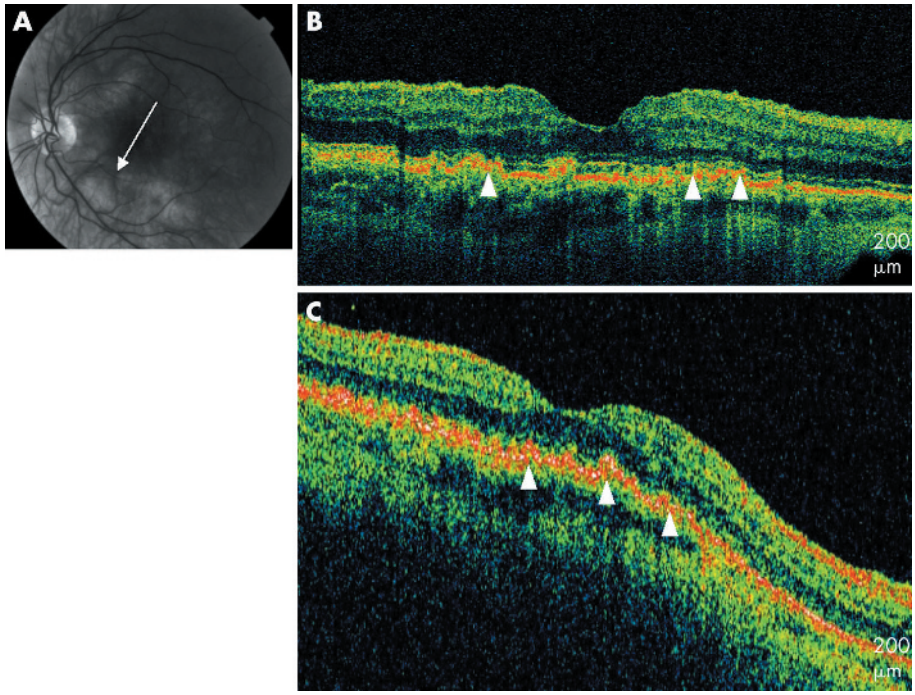

Figure 2 Soft drusen. (A) Red free fundus photograph of the left eye. (B) UHR-OCT image of the right eye with a saw toothed configuration of the RPE (white arrowheads). (C) StratusOCT image of the right eye shows a less distinct pattern (white arrowheads).

Five eyes (10%) with geographic atrophy were imaged. Generalised retinal thinning was apparent on UHR-OCT with higher than normal backscatter at the level of the choriocapillaris as a result of minimal light absorption by an atrophic RPE, making large choroidal vessels more evident (fig 7). Table 1 summarises the various types of nonexudative AMD imaged and the patterns observed. Select representative cases are presented below.

SELECTED CASE REPORTS

Drusen

Patient 1 (fig 1)

An 85 year old woman with confluent, soft drusen presented to the retina clinic. The UHR-OCT image shows multiple excrescences of the hyper-reflective RPE. The presence of less hyper-reflective material underneath these RPE elevations is observed, consistent with accumulation of drusen material. Above these excrescences, the overlying photoreceptors, including highly reflective photoreceptor inner/outer segment junction, appear compressed. The inner retinal layers appear generally intact. The outer retinal layers are less well defined on StratusOCT.

Patient 2 (fig 2)

A fundus photograph of a 74 year old woman with drusen is shown. The UHR-OCT image shows a saw toothed pattern of the RPE overlying moderately reflective drusen material. As with the previous case, overlying this wrinkled area of RPE,

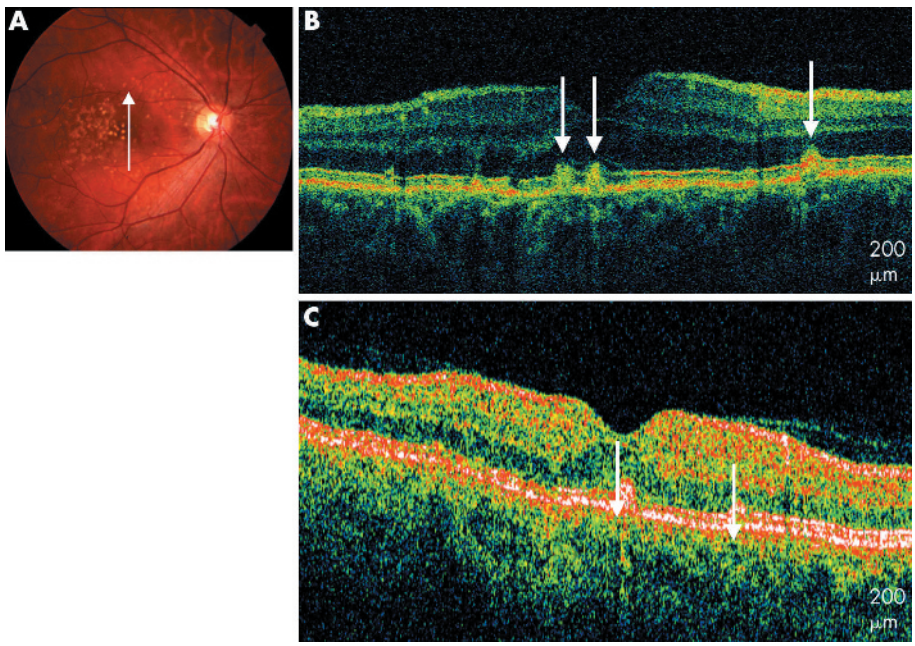

Figure 3 Soft and hard drusen. (A) Colour fundus photograph of the right eye. (B) UHR-OCT image of the right eye shows discrete hyper-reflective and moderately reflective nodules (white arrows). (C) StratusOCT image of the right eye shows less distinct accumulations (white arrows).

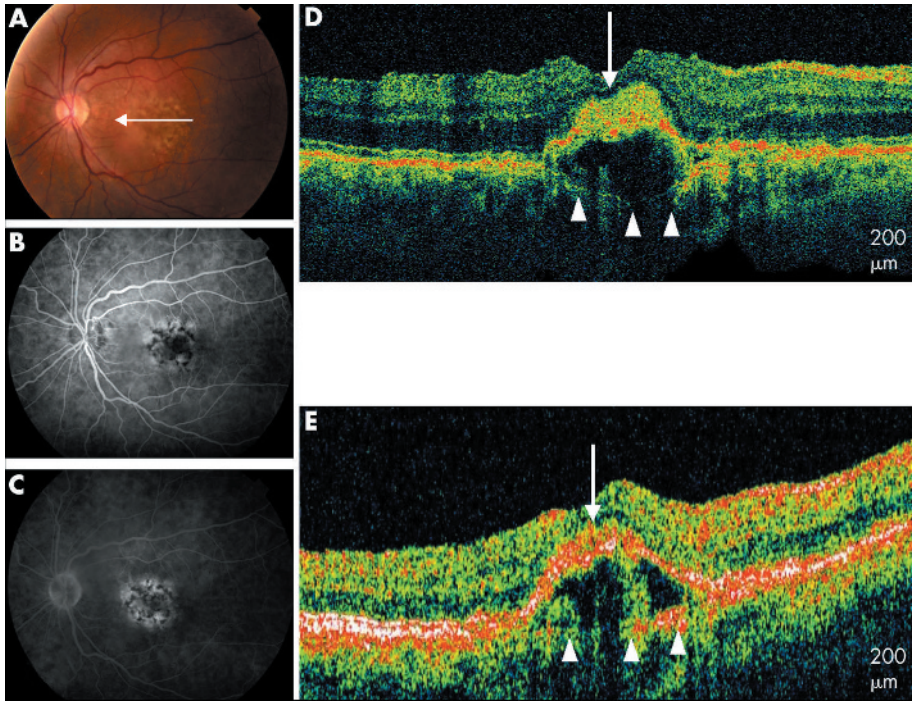

Figure 4 Soft drusen. (A) Colour fundus photograph of the left eye. (B) and (C) Early and late fluorescein angiogram of the left eye shows staining of drusen. (D) UHR-OCT image of the left eye with moderately reflective material penetrating the RPE (white arrow) overlying a pigment epithelial detachment. Bruch's membrane is visible beneath the low scattering PED (white arrowheads). (E) StratusOCT image of the left eye also shows Bruch's membrane (white arrowheads) below the PED.

the photoreceptors appear thinned or compressed. The highly reflective junction between the inner and outer photoreceptor segments is clearly distinguished on UHR-OCT. The RPE elevations are present but less distinct on the StratusOCT image.

Patient 3 (fig 3)

The fundus photograph of a 55 year old man with drusen is shown. The UHR-OCT image shows discrete nodules of highly reflective and moderately reflective material. Unlike the previous cases described, the RPE layer is not clearly defined in the area of these nodules. There appears to be discontinuity of the RPE where there is accumulation of material. The corresponding fundus photograph shows a few hard drusen scattered around the fovea that may correspond to the OCT findings. These nodules are not as well defined on the StratusOCT image.

Drusenoid pigment epithelial detachment

Patient 4 (fig 4)

A 79 year old woman with soft, confluent drusen presented to the retina service. Her UHR-OCT image shows elevation of

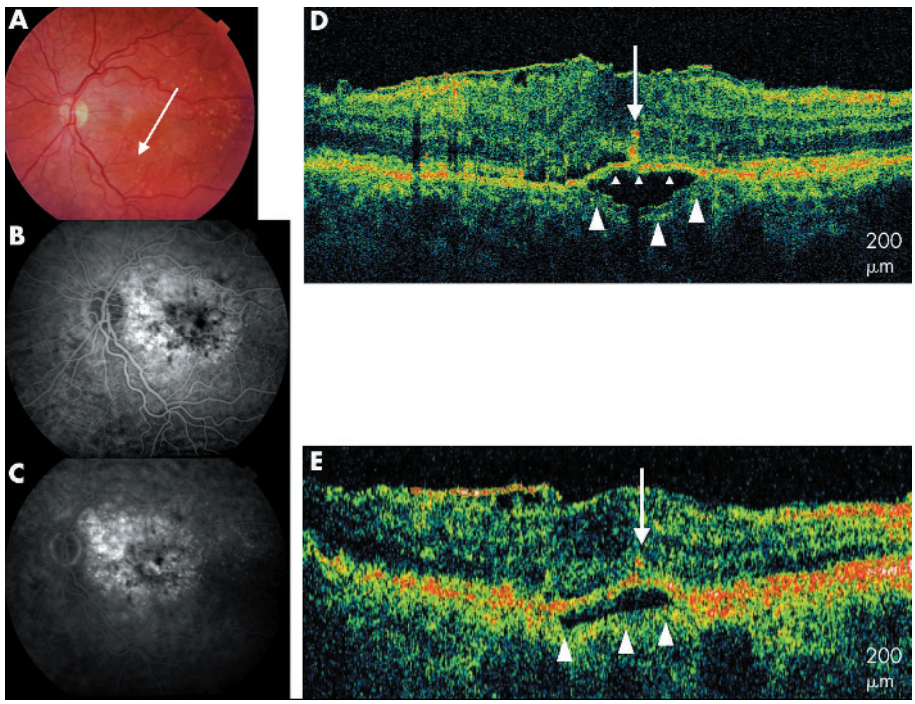

Figure 5 Soft drusen. (A) Colour fundus photograph of the left eye with drusen. (B) and (C) Early and late fluorescein angiogram of the left eye shows staining of drusen. (D) UHR-OCT shows a drusenoid pigment epithelial detachment with a splitting in Bruch's membrane to reveal the inner layer of Bruch's membrane (small arrowheads) and the outer layer of Bruch's membrane (large arrowheads). RPE migration is also seen (white arrow). (E) Stratus OCT image also shows a retinal pigment epithelial detachment with the outer part Bruch's membrane below the low scattering PED (large arrowheads).

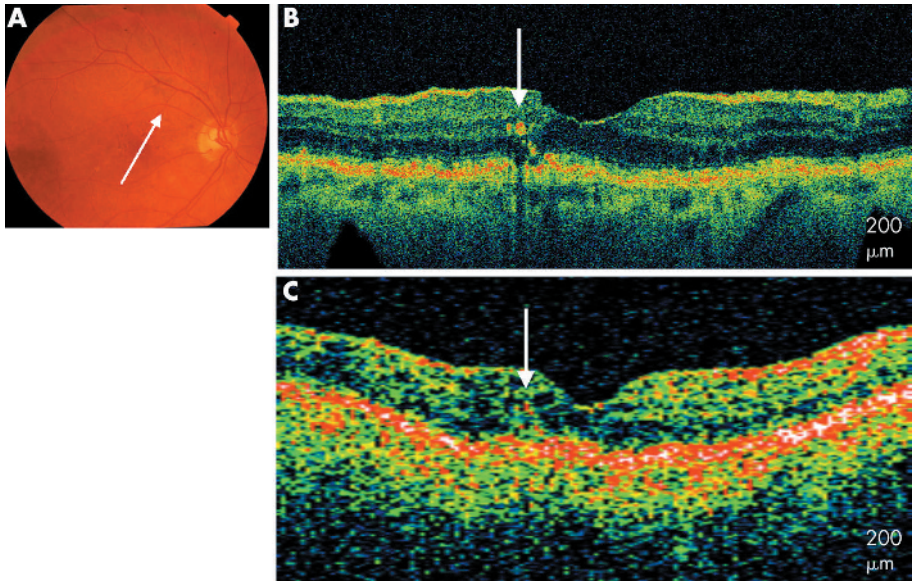

Figure 6 Drusen and RPE changes. (A) Colour fundus photograph of the right eye. (B) UHR-OCT image of the right eye with a hyper-reflective stalk protruding into the inner retinal layers (white arrow). (C) StratusOCT image of the right eye shows less distinct RPE migration into the inner retinal layers (white arrow).

the RPE overlying an optically low scattering area, consistent with an RPE detachment or a large druse. A thin reflective line present at the base of this fluid is consistent with Bruch's membrane. It is known that large confluent drusen can form pigment epithelial detachments without an underlying CNV. However, disruptions are seen within the overlying RPE with less reflective areas seemingly penetrating the RPE into the subretinal space with compression of the photoreceptor layer. Perhaps these areas reflect part of an early CNV. Early, mid, and late phase fluorescein angiography shows areas of blocked fluorescence alternating with areas of early hyperfluorescence that stain later.

Patient 5 (fig 5)

An 82 year old woman with a history of non-exudative AMD presented to the retina service for follow up. UHR-OCT image of the left eye reveals a small detachment of the RPE. Bruch's membrane is well visualised with a visible splitting of the moderately reflective inner Bruch's membrane from the moderately reflective outer Bruch's membrane above and below the low scattering hyporeflective fluid. Highly reflective particles present in the inner retinal layers probably represent RPE migration.[25] A RPE detachment is also seen on the Stratus OCT image but in less detail. An epiretinal membrane is seen on both the UHR-OCT and Stratus OCT image.

RPE changes

Patient 6 (fig 6)

A 79 year old woman with drusen and RPE changes presented to the retina service. The UHR-OCT image shows areas of RPE clumping alternating with areas of thinning within the anatomical confines of the RPE. Also apparent are multiple areas of hyper-reflective particles, perhaps consis-

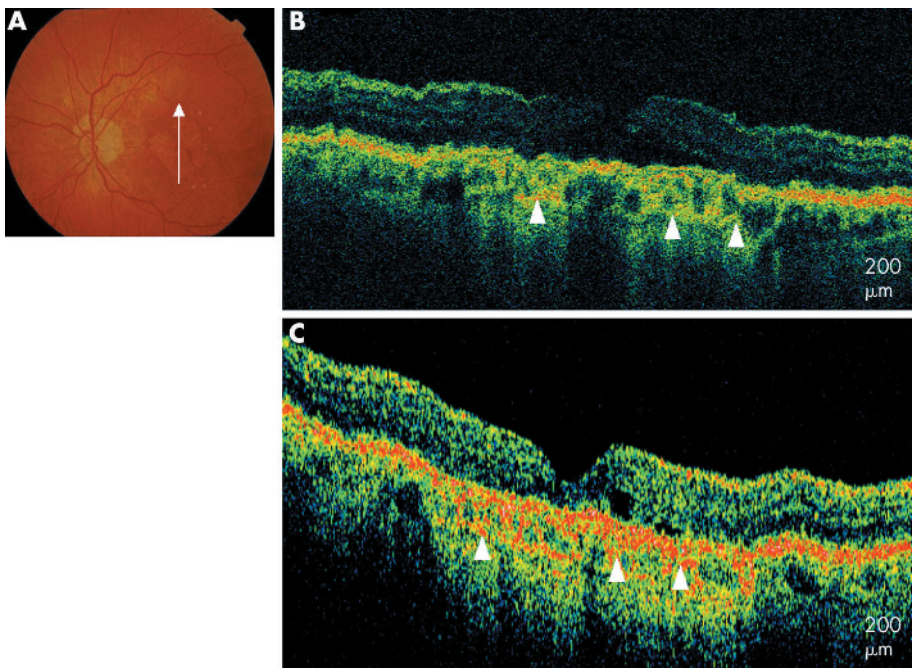

Figure 7 Geographic atrophy. (A) Colour fundus photograph of the left eye. (B) UHR-OCT image of the left eye with generalised retinal thinning, hyporeflectivity of the RPE, and prominent choroidal vessels (white arrowheads). (C) StratusOCT image of the left eye shows a similar pattern in less detail (white arrowheads).

Table 1 Forms of non-exudative age related macular degeneration imaged by ultrahigh optical coherence tomography

	No of eyes	%
Drusen		
Distinct RPE excrescences	15	29
Saw tooth pattern of RPE	8	15
Nodular	13	25
Retinal pigment epithelial changes		
With RPE cell migration	4	8
Without RPE cell migration	4	8
Drusenoid pigment epithelial detachment	3	6
Geographic atrophy	5	10

tent with RPE cells,[25] deposited within the inner nuclear and photoreceptor layers. These findings are less apparent on StratusOCT.

DISCUSSION

UHR-OCT images of ~3 μm axial resolution provide unprecedented morphological detail of macular pathologies.[16 17] We have developed a UHR-OCT imaging system and performed an observational case series of patients with a clinical diagnosis of dry or non-exudative AMD. Images of drusen, RPE changes, and drusenoid pigment epithelial detachment were presented.

Three patterns were observed in eyes with a diagnosis of drusen. Many eyes had components of all three categories. Soft drusen appeared as localised excrescences of the highly reflective RPE layer on UHR-OCT. Underneath these focal elevations were accumulations of less reflective material, presumably beneath the RPE either between the RPE and Bruch's membrane or within the inner layer of Bruch's membrane. A similar but clearly distinct pattern of RPE excrescences was also observed among those eyes with a clinical diagnosis of drusen. The hyper-reflective RPE in these eyes appeared to be elevated above excrescences in very close approximation, resembling a saw toothed pattern and perhaps representing a wrinkling or bunching of the RPE. The saw toothed pattern may represent motion artefact during image capture. However, a similar pattern was seen by StratusOCT, which supports consistency of the pattern. The pattern may be secondary to wrinkling of the internal limiting membrane at the vitreoretinal interface.

Drusen also had a third distinct appearance by UHR-OCT. These discrete nodules of highly and moderately reflective material with loss of a continuous RPE could represent hard drusen. With all three patterns, Bruch's membrane was difficult to identify because of the highly reflective RPE adjacent to this layer. Above the focal excrescences, the hyper-reflective junction between the inner and outer segments was elevated, with overlying compression of the outer retinal layers including the photoreceptors. Histological studies of eyes with drusen have shown photoreceptor cell degeneration, the severity of which was determined by the degree of photoreceptor layer thinning.[5]

Some patients also exhibited irregularities in the inner retinal layers. For example, the fundus photograph of patient 6 is consistent with RPE mottling and non-geographic RPE atrophic changes. The UHR-OCT revealed areas of hyper-reflective RPE clumping within the expected location of the RPE. Notable are the hyper-reflective particles deposited in the photoreceptor, inner nuclear, and inner plexiform layers. These accumulations might represent degenerated RPE cells.[25]

Interestingly, some patients with clinically dry changes were found to exhibit evidence of early exudative macular degeneration. Figure 4 shows a patient with clinically non-exudative AMD on biomicroscopy. UHR-OCT shows what looks like a pigment epithelial detachment with a focal area of elevation of the pigment epithelium overlying an optically low scattering space. Interestingly, the image shows an area of RPE disruption with the appearance of hyper-reflective material invading the subretinal space above the RPE. This is similar to the appearance of angiographically proved choroidal neovascular membranes described previously on OCT as a thickening and fragmentation of the RPE in association with subretinal fluid.[26] Fluorescein angiography in this patient did not show any evidence of choroidal neovascularisation (fig 4). Choroidal neovascular membranes may exist beyond clinical and angiographic detection. Evidence is supported by studies performed on postmortem pathological specimens.[27] In 19 of 210 eyes with diffuse drusen, Green *et al* detected the presence of early neovascularisation.[6]

The ability to detect early exudative changes with UHR-OCT becomes increasingly more important as new treatments continue to develop. Present therapy is directed towards the obliteration of clinically evident, angiographically established choroidal neovascularisation (CNV). With the introduction of anti-angiogenic therapy for the inhibition of CNV, in particular anti-vascular endothelial growth factor (VEGF) preparations, new challenges arise as the role or indications for these products have yet to be defined.[7] As treatment practices continue to evolve, perhaps earlier intervention would prove beneficial before sight threatening tissue destruction takes place. Given the increased resolution available with UHR-OCT, perhaps earlier indications for treatment can be identified. UHR-OCT may also be useful in monitoring regression of the new blood vessel growth. Further study is indicated for the follow up of patients with apparently subclinical CNV to establish a natural history of progression to clinically apparent CNV.

In summary, UHR-OCT provides cross sectional images of dry AMD with unprecedented resolution and detail. The notion that AMD represents a progression from early dry changes to more vision threatening advanced AMD is well established, but the pathogenesis is far from being fully elucidated. The images attainable with UHR-OCT are promising with regards to further understanding the pathogenesis of this disease. With new therapies on the horizon, UHR-OCT may be an integral tool for the management decisions involved in the treatment of patients with AMD.

Authors' affiliations

C G Pieroni, A J Witkin, A Chan, H Ishikawa, E Reichel, J S Duker, New England Eye Center, Tufts-New England Medical Center, Tufts University, Boston, MA, USA
T H Ko, J G Fujimoto, Department of Electrical Engineering and Computer Science and Research Laboratory of Electronics, Massachusetts Institute of Technology, Cambridge, MA, USA
J S Schuman, UPMC Eye Center, Department of Ophthalmology, University of Pittsburgh School of Medicine, Pittsburgh, PA, USA

Supported in part by NIH contracts RO1-EY11289-16, R01-EY13178, and P30-EY13078, NSF contract ECS-0119452, Air Force Office of Scientific Research contract F49620-98-1-0139, Medical Free Electron Laser Program contract F49620-01-1-0186 and by Carl Zeiss Meditec.

Competing interests: JGF and JSS receive royalties from intellectual property licensed by MIT to Carl Zeiss Meditec. JGF and JSS receive research support from Carl Zeiss Meditec.

REFERENCES

1 **Klaver CC**, Wolfs RC, Vingerling JR, *et al*. Age-specific prevalence and causes of blindness and visual impairment in an older population: the Rotterdam Study. *Arch Ophthalmol* 1998;**116**:653–8.

2 **Klein R**, Klein BE, Jensen SC, *et al*. The five-year incidence and progression of age-related maculopathy: the Beaver Dam Eye Study. *Ophthalmology* 1997;**104**:7–21.
3 **Klein R**, Klein BE, Tomany SC, *et al*. Ten-year incidence and progression of age-related maculopathy: The Beaver Dam Eye Study. *Ophthalmology* 2002;**109**:1767–79.
4 **Bressler SB**, Maguire MG, Bressler NM, *et al*. Relationship of drusen and abnormalities of the retinal pigment epithelium to the prognosis of neovascular macular degeneration. The Macular Photocoagulation Study Group. *Arch Ophthalmol* 1990;**108**:1442–7.
5 **Sarks JP**, Sarks SH, Killingsworth MC. Evolution of soft drusen in age-related macular degeneration. *Eye* 1994;**8**(Pt 3):269–83.
6 **Green WR**, Enger C. Age-related macular degeneration histopathologic studies. The 1992 Lorenz E Zimmerman Lecture. *Ophthalmology* 1993;**100**:1519–35.
7 **Gragoudas ES**, Adamis AP, Cunningham ET Jr, *et al*. Pegaptanib for neovascular age-related macular degeneration. *N Engl J Med* 2004;**351**:2805–16.
8 **Bressler SB**, Pieramici DJ, Koester JM, *et al*. Natural history of minimally classic subfoveal choroidal neovascular lesions in the treatment of age-related macular degeneration with photodynamic therapy (TAP) investigation: outcomes potentially relevant to management—TAP report No 6. *Arch Ophthalmol* 2004;**122**:325–9.
9 **Blinder KJ**, Bradley S, Bressler NM, *et al*. Effect of lesion size, visual acuity, and lesion composition on visual acuity change with and without verteporfin therapy for choroidal neovascularization secondary to age-related macular degeneration—TAP and VIP report No 1. *Am J Ophthalmol* 2003;**136**:407–18.
10 **Barbazetto I**, Burdan A, Bressler NM, *et al*. Photodynamic therapy of subfoveal choroidal neovascularization with verteporfin: fluorescein angiographic guidelines for evaluation and treatment—TAP and VIP report No 2. *Arch Ophthalmol* 2003;**121**:1253–68.
11 **Blumenkranz MS**, Bressler NM, Bressler SB, *et al*. Verteporfin therapy for subfoveal choroidal neovascularization in age-related macular degeneration: three-year results of an open-label extension of 2 randomized clinical trials—TAP Report No 5. *Arch Ophthalmol* 2002;**120**:1307–14.
12 **Bressler NM**. Photodynamic therapy of subfoveal choroidal neovascularization in age-related macular degeneration with verteporfin: two-year results of 2 randomized clinical trials-tap report 2. *Arch Ophthalmol* 2001;**119**:198–207.
13 **Treatment Of Age-Related Macular Degeneration With Photodynamic Therapy (TAP) Study Group**. Photodynamic therapy of subfoveal choroidal neovascularization in age-related macular degeneration with verteporfin: one-year results of 2 randomized clinical trials—TAP report. *Arch Ophthalmol* 1999;**117**:1329–45.
14 **Macular Photocoagulation Study Group Argon laser photocoagulation for neovascular maculopathy**. Five-year results from randomized clinical trials. *Arch Ophthalmol* 1991;**109**:1109–14.
15 **Macular Photocoagulation Study Group**. Krypton laser photocoagulation for neovascular lesions of age-related macular degeneration. Results of a randomized clinical trial. *Arch Ophthalmol* 1990;**108**:816–24.
16 **Drexler W**, Morgner U, Ghanta RK, *et al*. Ultrahigh-resolution ophthalmic optical coherence tomography. *Nat Med* 2001;**7**:502–7.
17 **Drexler W**, Sattmann H, Hermann B, *et al*. Enhanced visualization of macular pathology with the use of ultrahigh-resolution optical coherence tomography. *Arch Ophthalmol* 2003;**121**:695–706.
18 **Pons ME**, Garcia-Valenzuela E. Redefining the limit of the outer retina in optical coherence tomography scans. *Ophthalmology* 2005;**112**:1079–85.
19 **Anger EM**, Unterhuber A, Hermann B, *et al*. Ultrahigh resolution optical coherence tomography of the monkey fovea: Identification of retinal sublayers by correlation with semithin histology sections. *Exp Eye Res* 2004;**7**:1117–25.
20 **Hee MR**, Izatt JA, Swanson EA, *et al*. Optical coherence tomography of the human retina. *Arch Ophthalmol* 1995;**113**:325–32.
21 **Huang D**, Swanson EA, Lin CP, *et al*. Optical coherence tomography. *Science* 1991;**254**:1178–81.
22 **Ko TH**, Fujimoto JG, Duker JS, *et al*. Comparison of ultrahigh and standard resolution optical coherence tomography for imaging of macular pathology and repair. *Ophthalmol* 2004;**111**:2033–43.
23 **American National Standards Institute**. *Safe use of lasers*. New York: American National Standards Institute, 1993.
24 **Swanson EA**, Izatt JA, Hee MR, *et al*. In vivo retinal imaging by optical coherence tomography. *Optics Lett* 1993;**18**:1864–6.
25 **Zacks DN**, Johnson MW. Transretinal pigment migration: an optical coherence tomography study. *Arch Ophthalmol* 2004;**122**:406–7.
26 **Hee MR**, Baumal CR, Puliafito CA, *et al*. Optical coherence tomography of age-related macular degeneration and choroidal neovascularization. *Ophthalmology* 1996;**103**:1260–70.
27 **Sarks SH**. New vessel formation beneath the retinal pigment epithelium in senile eyes. *Br J Ophthalmol* 1973;**57**:951–65.